

# VIBRATION POWER GENERATION WITH PIEZOELECTRIC ELEMENT USING COUPLING WITH CYLINDRICAL SOUND FIELD ENCLOSED BY END PLATES HAVING DIFFERENT THICKNESS

B.Eng. Ohba Y.<sup>1</sup> and Prof. D.Eng. Moriyama H.<sup>2</sup>

Course of Mechanical Engineering, Graduate School of Tokai University, Japan<sup>1</sup>

Department of Prime Mover Engineering, Tokai University, Japan<sup>2</sup>

tennis-zuki.555@ezweb.ne.jp

**Abstract:** This paper describes the electricity generation characteristics of a new energy-harvesting system with piezoelectric elements. The proposed system is composed of a rigid cylinder and thin plates at both ends. The piezoelectric elements are installed at the centers of both plates, and one side of each plate is subjected to a harmonic point force. In this system, vibration energy is converted into electrical energy via electro-mechanical coupling between the plate vibration and piezoelectric effect. In addition, the plate vibration excited by the point force induces a self-sustained vibration at the other plate via mechanical-acoustic coupling between the plate vibration and an internal sound field into the cylindrical enclosure. Therefore, the electricity generation characteristics should be considered as an electro-mechanical-acoustic coupling problem. Actually, the plate on the excitation side is lower than that on the non-excitation side in the natural frequency because of the influence of a vibrator to apply the point force to the plate, so that both natural frequencies are not identical and the effect of mechanical-acoustic coupling is not clarified very well. Then both frequencies are close by tuning the natural frequency due to thinning the plate on the non-excitation side. As a result, it is expected that the electricity generation characteristics are improved by promoting mechanical-acoustic coupling in comparison with the inherent situation.

**Keywords:** MECHANICAL-ACOUSTIC COUPLING, CYLINDRICAL STRUCTURE, THIN END PLATE, INTERNAL SOUND FIELD, PLATE VIBRATION, NATURAL FREQUENCY, PIEZOELECTRIC ELEMENT

## 1. Introduction

To deal with a depletion of fossil fuels and to materialize a low-carbon society, not only the improvement of energy saving technologies but also the creation of new energy sources have been attempted in a lot of studies. Scavenging untapped vibration energy and converting it into usable electric energy via piezoelectric materials has attracted considerable attention and has been regarded as one of new energy sources<sup>1</sup>. Typical energy harvesters adopt a simple cantilever configuration to generate electric energy via piezoelectric materials, which are attached to or embedded in host structures, and the behavior is governed by electro-mechanical coupling phenomena.

To enhance the conversion efficiency, two methods have been adopted in many cases: the optimization of piezoelectric element placement and the use of a large element or many elements. To further improve the conversion efficiency, a mechanical impedance matching method, which was derived from using spacers between the piezoelectric element and beam structure and tuning for the size of the piezoelectric element, was proposed<sup>2</sup>. These structural vibrations are caused by vibrators and various power sources. For instance, a self-sustained oscillation caused by placing a plate into a flow whose critical velocity was overpassed (so-called 'fluttering') is a well-known phenomenon. To utilize such a fluttering phenomenon for energy-harvesting, the plate on which the piezoelectric elements were arranged was used, and the effect of their arrangement along the flow axis was considered. Then an optimization of the arrangement was performed among some positions and dimensions of piezoelectric elements<sup>3</sup>.

To develop a new electricity generation system using mechanical-acoustic coupling, we adopt analytical and experimental models that consist of cylindrical structure and both end plates, because the vibration area of the model on which piezoelectric elements can be installed is twice as large as that in the case of a single plate. The cylinder length is varied over a wide range while changing the plate thickness, while the harmonic point force is applied to one end plate and its frequency is selected to cause the plate to vibrate in the fundamental mode. The plate vibration induces electricity generation via electro-mechanical coupling with the piezoelectric effect of the surface-mounted piezoelectric element, while the plate vibration of the excitation side oscillates the other plate via mechanical-acoustic coupling. Consequently, the electro-mechanical-acoustic coupling problem must be considered and is estimated from the electric power caused by the electricity generation, the mechanical power supplied to the plate, and the

electricity generation efficiency that is derived from the ratio of both powers.

Actually, the plate on the excitation side is lower than that on the non-excitation side in the natural frequency because of the influence of a vibrator to apply the point force to the plate, so that both natural frequencies are not identical and the effect of mechanical-acoustic coupling is not clarified very well. Therefore, both frequencies are gotten closer by tuning the natural frequency due to thinning the plate on the non-excitation side, so that we verify that the performance of the proposed system is improved by promoting mechanical-acoustic coupling in comparison with the inherent situation.

## 2. Experimental apparatus and method

Figure 1 shows the configuration of the experimental apparatus used in this study. The structure consists of a steel cylinder with circular aluminum end plates. Plate 1 is subjected to the point force, whose frequency makes the plate excite in the (0,0) mode; and amplitude  $F$  is controlled to be 1 N, excited by a small vibrator. The position of the point force  $r_1$  is normalized by radius  $r_c$  and is set to  $r_1/r_c = 0.4$ . The thickness  $h_{c1}$  of plate 1 is fixed at 3.0 mm, whereas those of 2.5 and 3.0 mm are adopted for plate 2 to change vibration characteristics. The cylinder has an inner radius of 153 mm, and the length  $L$  can range from 500 to 2000 mm to emulate the analytical model.

In the excitation experiment, to estimate the mechanical power  $P_m$  supplied to plate 1 by the small vibrator, an acceleration sensor is installed near the position of the point force on plate 1, and  $P_m$  is predicted from the point force and acceleration  $a_1$ . The phase difference between the plate vibrations is also measured owing to the installation of the acceleration sensor at the same position on plate 2, resulting in significant effects on the mechanical-acoustic coupling. To estimate the internal acoustic characteristics, the sound pressure level in the cavity is measured using condenser microphones with a probe tube. The tips of the probe tubes are located near the plates and the cylinder wall, which are the approximate locations of the maximum sound pressure level when the sound field becomes resonant.

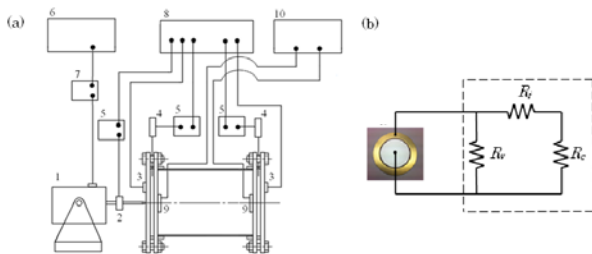
To perform the electricity generation experiment, the piezoelectric element is used. It is comprised of a piezoelectric part constructed of ceramics and an electrode part constructed of brass, which have radii  $r_p$  and  $r_b$  of 12.5 and 17.5 mm and thicknesses  $h_p$  and  $h_b$  of 0.23 and 0.30 mm, respectively. The piezoelectric elements are installed at the centers of both plates, as shown in

Fig.1(a). The electric power  $P_{e1}$  and  $P_{e2}$  generated by the expansion and contraction of the piezoelectric elements on plates 1 and 2 are discharged through the resistance circuit, which consists of three resistors having resistances  $R_v$ ,  $R_i$  and  $R_c$ , as shown in Fig. 1(b).  $R_v$  and  $R_i$  are the resistances of the voltmeter and ammeter, which are built-into the wattmeter, and are 2 M $\Omega$  and 2 m $\Omega$ , respectively; while  $R_c$  is the resistance of the resistor connected outside the wattmeter and is 97.5 k $\Omega$ . To grasp the effect of mechanical-acoustic coupling on energy harvesting, the electric power and other data are also measured without the cylinder (i.e. in the electricity generation under the vibration of only plate 1) and are estimated in comparison with those with cylinder. In such an estimation, electricity generation efficiency is used and is derived from the electric power normalized by the mechanical power  $P_m$  supplied to plate 1 by the vibrator. However, the electricity generation efficiencies, which are obtained from  $P_{e1}$ ,  $P_{e2}$ , and their total electric power  $P_e$ , are denoted by  $P_{em1}$ ,  $P_{em2}$ , and  $P_{em}$ , respectively.

### 3. Results and discussion

#### 3.1. Fundamental characteristics of electricity generation

Figure 2 shows the theoretical and experimental accelerations  $a_1$  at the excitation point as functions of the excitation frequency  $f$ . Before obtaining these results, we carried out experimental modal analysis and made sure of the natural frequency of plate 1. Then the actual condition adopts  $T_n = 10^8$  and  $R_n = 10^1$  to get closer to the experimental support condition<sup>4</sup>. Because this support condition brings the natural frequency to 280 Hz, the corresponding  $a_1$  reaches the peak at the natural frequency. However, the point force is applied to plate 1 via a stick whose natural frequency is shifted to a lower frequency region than that of plate 1 to avoid the effect on the (0,0) mode and higher-order modes. Therefore, the characteristics of the entire vibration system contain the behavior of the stick, so that such a variation in  $a_1$  never takes place in the actual results.



1: Vibration generator, 2: Load cell, 3: Acceleration sensor, 4: Condenser microphone, 5: Amplifier, 6: Multifunction generator, 7: Power supply, 8: FFT analyzer, 9: Piezoelectric element, 10: Power meter

Fig.1 Experimental apparatus.

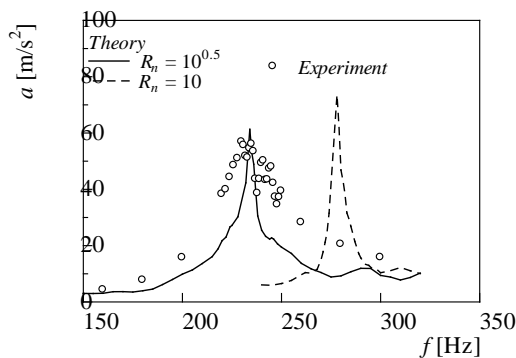


Fig.2 Acceleration as function of excitation frequency.

Since it is difficult to theoretically express the actual situation, a theoretical consideration is attempted by shifting the natural frequency of plate 1 to the experimental peak frequency. The theoretical  $a_1$  has peaks at  $f = 234$  and 280 Hz that are derived from  $R_n = 10^{0.5}$  and  $10^1$ , respectively, and the experimental  $a_1$  is maximized around  $f = 230$  Hz.

The cylinder and plate 2 are added to the above theoretical and experimental models which were introduced in the previous section, i.e. they are models as shown in Figs. 1. In the analytical model, the dimensions and so on of plate 2 are identical to those of plate 1, the support condition adopts  $T_n = 10^8$  and  $R_n = 10^1$  in both plates, and the point force  $F$  is set to 1 N. The cylinder has the same radius as that of plates 1 and 2, and its length  $L$  ranges from 100 to 2000 mm.

Figure 3 shows the sound pressure level  $L_{pv}$ , which is averaged over the entire volume of the cavity and is maximized at each  $L$  when  $h_{c1}$ ,  $h_{c2}$ , and  $f$  are set to 3 mm and 280 Hz, respectively, and the phase  $\alpha_2$  ranges from 0 to 180° as functions of  $L$ . The theoretical level  $L_{pv}$  peaks at 610, 1230, and 1840 mm. The peaks are caused by the promotion of mechanical-acoustic coupling between the plate vibration and acoustic modes. Then the acoustic modes are the (0,0,1), (0,0,2), and (0,0,3) modes whose plane modal shape is similar to that of plate vibration mode (0,0). To validate these theoretical results, the sound pressure levels  $L_{p1}$  and  $L_{p2}$ , which are measured near plates 1 and 2, are also indicated. The experimental peaks occur around the lengths where  $L_{pv}$  peaks, whereas  $L_{p1}$  decreases remarkably around  $L = 950$  and 1600 mm in the process of shifting acoustic modes because of a changing  $L$ .

To consider the effect of mechanical-acoustic coupling on electricity generation characteristics, Fig. 4 shows the experimental accelerations  $a_1$  and  $a_2$  of plates 1 and 2 as functions of  $L$  under the above coupling. Since plate 1 is excited at  $f = 280$  Hz via the stick connected with the vibrator,  $a_1$  remains low and almost constant over the entire range of  $L$ , having small increases at  $L = 620$ , 1250, and 1880 mm. These results can be also predicted from those in Fig. 2. On the other hand, the cylindrical sound field connecting with

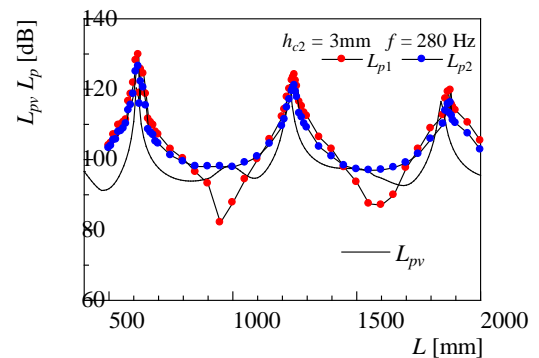


Fig.3 Sound pressure level as functions of cylinder length.

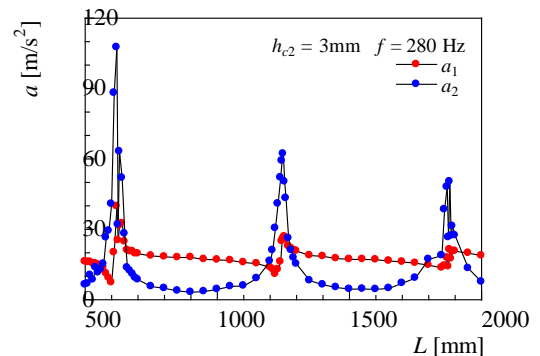


Fig.4 Acceleration as functions of cylinder length.

plate 1 is formed via mechanical-acoustic coupling, and plate 2 is excited by the sound field without the point force. As a result,  $a_2$  of plate 2 has specific peaks at  $L = 620, 1250,$  and  $1880$  mm, suppressed in the other ranges of  $L$ , because the natural frequency of plate 2 becomes  $280$  Hz. Figure 5 shows the voltages  $v_1$  and  $v_2$  based on the electricity generations of plates 1 and 2 as functions of  $L$ .  $v_1$  and  $v_2$  are directly proportional to  $a_1$  and  $a_2$ , respectively, depending on the in-plane strain of the plate that is determined by the out-of-plane deflection of the plate. Therefore,  $v_1$  and  $v_2$  have a tendency that is similar to that of  $a_1$  and  $a_2$ ; in particular,  $v_2$  is much larger than  $v_1$  at  $L = 620$  mm, at which coupling with the  $(0,0,1)$  mode is promoted, as well as the behavior of  $a_1$  and  $a_2$ .

The electricity generation efficiencies  $P_{em1}$  and  $P_{em2}$  are calculated from the relationship between electric power via the piezoelectric element and mechanical power supplied to plate 1. They are shown with changing  $L$  in Fig. 6. They are derived from the above results so that  $P_{em1}$  of plate 1 remains almost constant over the entire range of  $L$ , and  $P_{em2}$  of plate 2 increases greatly at  $L = 620, 1250,$  and  $1880$  mm.

### 3.2. Mechanical-acoustic coupling with plates having different thickness

To consider characteristics of the electricity generation using mechanical-acoustic coupling in the previous section, the analytical and experimental models, in which the thicknesses of plates 1 and 2 are identical, were adopted as the fundamental model. Then plate 1 was subjected to the point force of the natural frequency in its free vibration, so that the acceleration of plate 1 was suppressed in comparison with that of plate 2 since the actual natural frequency of plate 1 affected by the small vibrator was lower than the excitation frequency. Here, plate 1 is excited in such an actual natural frequency and the thickness of plate 2 is adjusted to get its natural frequency closer to the actual natural frequency.

Figure 7 shows the and experimental sound pressure levels  $L_{p1}$  and  $L_{p2}$  as functions of the cylinder length  $L$ , when both thicknesses remain  $3.0$  mm and the excitation frequency  $f$  is set to  $230$  Hz by referring to Fig. 2.  $L_{p1}$  and  $L_{p2}$  are also maximized around  $L = 745$

and  $1485$  mm by the promotion of coupling as well as Fig.3, whereas their lengths are longer than those in Fig. 3 due to bringing the excitation frequency to the lower range. Under the function of mechanical-acoustic coupling, the acceleration  $a_1$  and  $a_2$  behaves as shown in Fig. 8. Although the acceleration also increases around the above specific lengths,  $a_1$  is considerably larger than  $a_2$ , with the result that these tendencies are opposite to those in Fig. 4. This is because the natural frequency of plate 1 is closer to  $f$  than that of plate 2. If  $f$  were gotten closer to the natural frequency of plate 2, mechanical-acoustic coupling would be promoted and  $a_2$  would be larger than the present situation.

Then the same experiment is carried out with setting  $f$  to  $235$  Hz and the results of the sound pressure level are shown in Fig. 9. In this case,  $L_{p2}$  remains large and almost constant over the entire range of  $L$ , whereas  $L_{p1}$  has relatively large variation in comparison with  $L_{p2}$  and approaches  $L_{p1}$  at  $L = 1500$  mm, increasing rapidly and extremely. These characteristics are completely different from those in Figs. 3 and 7. Figure 10 shows  $a_1$  and  $a_2$  as functions of the cylinder length  $L$  under the same situation.  $a_1$  and  $a_2$  change greatly with  $L$  and have the respective periods. Therefore, these characteristics are also different from those in Figs. 4 and 8 and have opposite tendencies in the ranges of  $500$  mm to  $750$  mm, of  $1000$  mm to  $1450$  mm, and of  $1750$  mm to  $2000$  mm, respectively. However,  $a_1$  remains large and  $a_2$  increases sharply at  $L = 1500$  mm, and then both accelerations increase  $L = 700$  mm, deviating from the above tendencies. These mean that the promotion of coupling occur not only at  $L = 1500$  mm but also at  $L = 700$  mm, at which we can make sure of small peaks of  $L_{p1}$  and  $L_{p2}$ .

### 3.3. Improvement of electricity generation characteristics

As described in the above sections, the vibrations characteristics of plates 1 and 2 are strongly affected by the shift in the natural frequency of plates 2 and the excitation frequency. It is natural that such an effect is reflected in the electricity generation characteristics. Here, the section takes up the three cases: the respective thickness  $h_{c2}$  of plate 2 are  $3.0$  mm when the excitation frequency  $f$  is  $280$  Hz,  $h_{c2} = 3.0$  mm when  $f = 230$  Hz, and  $h_{c2} = 2.5$  mm when  $f = 235$  Hz.

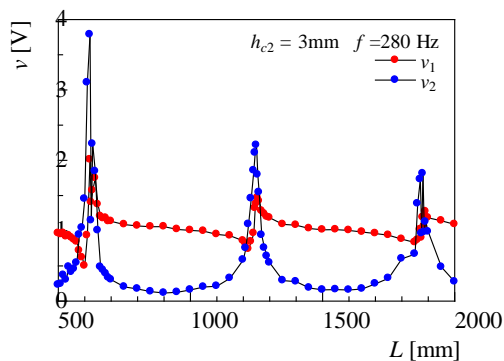


Fig.5 Voltage as functions of cylinder length.

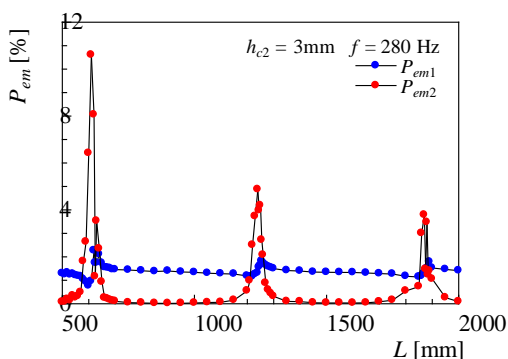


Fig.6 Electricity generation efficiency as function of cylinder length.

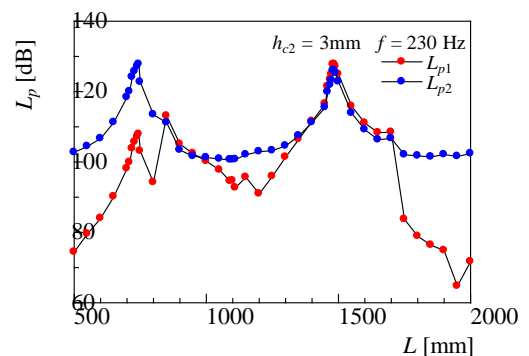


Fig.7 Sound pressure level as functions of cylinder length.

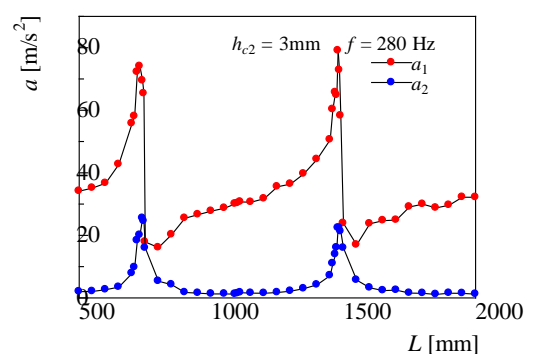


Fig.8 Acceleration as functions of cylinder length.

Figure 11 shows the electricity generation efficiency  $P_{em}$ , which is obtained from total electric power  $P_e$ , as functions of the cylinder length  $L$ . In the case of  $h_{c2} = 3.0$  mm and  $f = 280$  Hz,  $P_{em}$  peaks at  $L = 620, 1250,$  and  $1880$  mm by the derivation of  $P_{em2}$  of plate 2 and remains almost constant and low in the other ranges of  $L$  by the derivation of  $P_{em1}$  of plate 1, as shown in Fig. 6. The efficiency peaks decrease with shifting the acoustic modes, such as the (0,0,1), (0,0,2), and (0,0,3) modes. When  $h_{c2} = 3.0$  mm and  $f = 230$  Hz,  $P_{em}$  peaks at  $L = 740$  and  $1480$  mm where mechanical-acoustic coupling is promoted, whereas  $P_{em}$  is occupied by  $P_{em1}$  and its peaks do not decrease with shifting the acoustic modes, because this coupling is controlled by the vibration of plate 1. Moreover, when  $h_{c2} = 2.5$  mm and  $f = 235$  Hz,  $P_{em}$  remains large over the entire range of  $L$ , because this coupling is controlled by the vibrations of both plates. In particular,  $P_{em}$  increases greatly in the vicinities of the specific lengths where the accelerations  $a_1$  and  $a_2$  increase simultaneously as shown in Fig. 10 and exceeds greatly  $P_{em}$  on the other conditions.

Figure 12 shows variations in  $P_e$ , which is employed to obtain  $P_{em}$ , with  $L$  on the above condition. In the cases of  $h_{c2} = 3.0$  mm and  $f = 230$  and  $280$  Hz, variations in  $P_e$  are similar to that in  $P_{em}$ . The maximum  $P_{em}$  at  $f = 230$  Hz is somewhat less than that at  $f = 280$  Hz, because the mechanical power  $P_m$  supplied to plate 1 by the vibrator is suppressed due to the discrepancy between the natural and excitation frequencies. However, the maximum  $P_e$  at  $f = 230$  Hz is larger than that at  $f = 280$  Hz, because the electricity generation characteristics depend on the vibration of plate 1, whose natural frequency is close to the excitation frequency. On the other hand,  $P_e$  at  $h_{c2} = 2.5$  mm and  $f = 235$  Hz exceeds considerably those on the other conditions, as well as  $P_{em}$ , and the maximum  $P_e$  is obtained at  $L = 1500$  mm. This is because mechanical-acoustic coupling is strongly promoted, having significant contribution of both plate vibrations whose natural frequencies are the closest to the excitation frequency among all conditions.

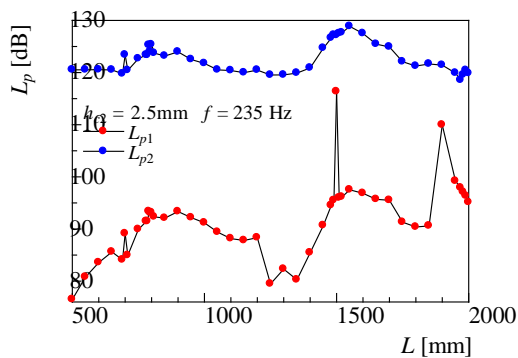


Fig.9 Sound pressure level as functions of cylinder length.

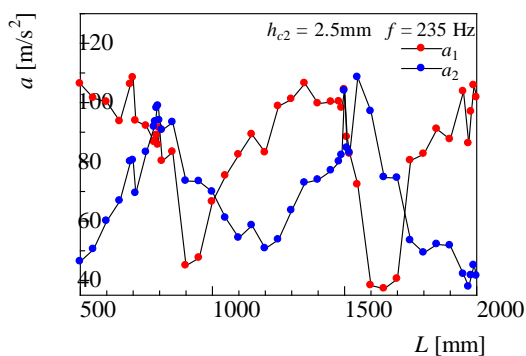


Fig.10 Acceleration as functions of cylinder length.

#### 4. Conclusion

In this study, a new electricity generation system, which consisted of a cylinder with circular end plates on which a piezoelectric element was installed at the center, was proposed. To improve the performance of the proposed system, the effect of mechanical-acoustic coupling on energy harvesting was considered by changing the plate thickness and the excitation frequency and was estimated from the electric power via the piezoelectric element, mechanical power supplied to the plate, and electricity generation efficiency.

The electric power increases by means of making the excitation frequency get closer to the natural frequency of the excitation side, which is considering the influence of a vibrator to apply the point force to the plate. In particular, it is effective measures that both plate vibrations contribute strongly to mechanical-acoustic coupling by getting the natural frequencies of both plates closer to the excitation frequency, so that the electric power and electricity generation efficiency are improved considerably.

#### References

- Anton S.R., H.A. Sodano, A review of power harvesting using piezoelectric materials (2003–2006), *Smart Materials and Structures*, 16, 2007, 1-21.
- Yamada K., H. Matsuhira, H. Utsuno, Improvement of efficiency of piezoelectric element attached to beam based on mechanical impedance matching, *J. Sound Vib.*, 333(1), 2014, 52-79.
- Piñeirua M., O. Doaré, S. Michelin, Influence and optimization of the electro desposition in a piezoelectric energy harvesting flag, *J. Sound Vib.*, 346, 2014, 200-215.
- Nishikawa K., H. Moriyama, Energy harvesting using vibro-acoustic coupling phenomenon, *MTM2013*, 18-20.09.2013, CD.

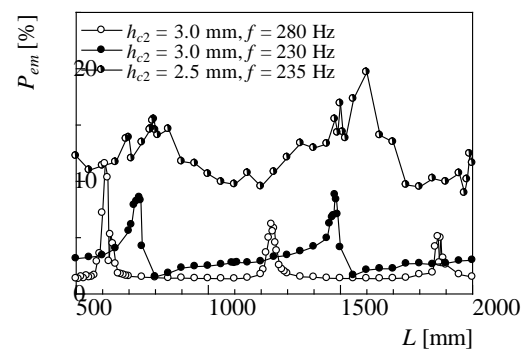


Fig.11 Electricity generation efficiency as function of cylinder length.

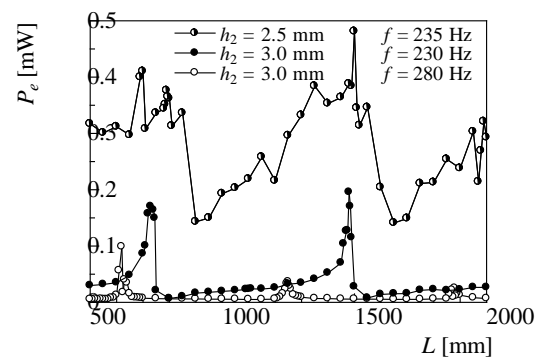


Fig.12 Electric power as function of cylinder length.